Engineering Properties of Overconsolidated Pleistocene Soils of Texas Gulf Coast

MICHAEL W. O'NEILL AND GIL YOON

Engineering soil properties, including undrained shear strength, overconsolidation ratio (OCR), coefficient of earth pressure at rest, Young's modulus, and cyclic degradation factors, obtained by various in situ and laboratory testing methods are presented for two Texas Gulf Coast sites. Soil deposition was deltaic, and preconsolidation occurred as a result of desiccation, producing local variability, as well as variability from site to site. The most comprehensively studied property, OCR, is in the range of 3 to 7 at Site A below a depth of 3 m, in which the soils to a depth of 8 m were formed in a pro-delta environment. Site B, at which the soils to a depth of about 11 m were formed in a backswamp environment several kilometers from Site A, indicated that OCR values are two to three times as high. Properties at Site A are probably appropriate for conservative geotechnical design at most sites in the geographical area.

This paper is concerned with the engineering properties of two Pleistocene terrace formations found along the Gulf Coast, generally west of the Mississippi River and north of the Rio Grande, exposed at the surface to about 100 km inland from the present coastline. Both formations have similar depositional histories. The lower formation, termed the Upper Lissie formation or Montgomery formation (the latter designation will be used here), was deposited on a gentle slope on an older Pleistocene formation during the Sangamon Interglacial Stage by streams and rivers near the existing coast, where numerous large and small river deltas developed. After deposition, the nearby sea level was lowered during the first Wisconsin Glacial Stage, producing desiccation and consolidation of the Montgomery soils, which consisted primarily of clays and silts. At the beginning of the Peorian Interglacial Stage, as the glaciers were retreating, the sea level returned to its previous level, producing a preconsolidation effect within the Montgomery formation. At the same time, rivers and streams produced sedimentary deposits on top of the slightly seaward-sloping Montgomery from the existing coastline to about 60 km inland from the present coastline. The resulting new formation, primarily a fresh-water deposit sloping toward the Gulf of Mexico, has characteristics typical of deltaic environments, including point bar, natural levee, backswamp, and pro-delta deposits within, beside, and at the termination of distributary channels. This formation is known as the Beaumont formation in Texas. After deposition, the nearby Gulf of Mexico receded by about 125 m once more during the late Wisconsin Glacial Stage, inducing desiccation in the Beaumont and redesiccating the underlying Montgomery. Finally, with the recession of the late Wisconsin glaciers, the sea level returned to its present level, leaving both formations preconsolidated through desiccation (*1,2*). A map of Beaumont-aged distributary channels within the Houston, Texas, area is shown in Figure 1 (*3*). Most of these channels became inactive and were covered by a few meters of clay during Recent times. Because of the differing depositional processes, Williams (*3*) has predicated that clays, now overconsolidated, that were deposited as backswamp soils have higher overconsolidation ratios (OCRs) and therefore have different properties from those that were deposited within or in front of microdeltas. The depositional process left thin seams of fine sand or silt within the primary deposits of clay in the Beaumont. Weathering of the Montgomery formation before deposition of the Beaumont leached some of the clay from the soil, resulting in soils near the surface of the Montgomery that are more silty and sandy than the soils of the Beaumont. The Beaumont-Montgomery contact is unconformable, and rather significant changes in water content, Atterberg limits and strength properties often occur there.

Desiccation produced a complex network of joints in both formations that were filled with solids during succeeding flooding events. This infilling restricted the return of the soil, through swelling, to its state of strain before desiccation, resulting in high values of the effective coefficient of earth pressure at rest, K_0. Al-Layla (*2*) characterized the clays as existing in "lumps" with an average of 2 to 4 mm between closed joints in each direction. Evidence that this process produced a "gilgai" structure (surface waves produced by wetting due to horizontally and vertically varying density of joints and resulting chemistry changes) in the present Beaumont formation is presented by Georghiou et al. (*4*). Mahar and O'Neill (*5*) surmised that this joint structure resulted in spacewise variable preconsolidation pressures over a few tenths of millimeters, with the highest capillary stresses (highest preconsolidation pressures) near the joint surfaces and the lowest in the interior of the blocks. Higher preconsolidation pressures should also exist in gilgai mounds, spaced 15 to 40 m apart, rather than in the troughs between the mounds. Therefore, not only are the Beaumont and Montgomery formations variable macroscopically, depending on the location of the point of investigation relative to distributary channels (Figure 1), but they may also be variable on a typical site scale because of systematically varying joint patterns (gilgai) and, on a microscale, because of variable capillary stresses and the presence of heterogeneous materials deposited within open joints and horizontally as seams. These characteristics influence the engineering properties.

Capillary stresses in the Beaumont were high enough to preconsolidate it through its entire thickness. Vertical effective stresses produced within the Montgomery by overburden loading from the Beaumont, which is 8 to 12 m thick within Houston, are considerably less than the capillary stresses produced by desiccation and loss of buoyancy at the base of the Montgomery. The Montgomery therefore remains preconsolidated for its entire thickness, about

Department of Civil and Environmental Engineering, University of Houston, Houston, Texas, 77204-4791.

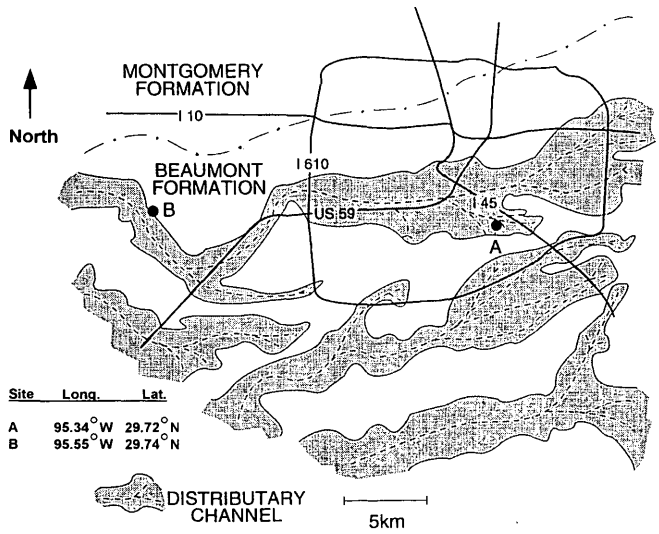

FIGURE 1 Location of distributary channels within Beaumont formation in the Houston, Texas, area (*3*).

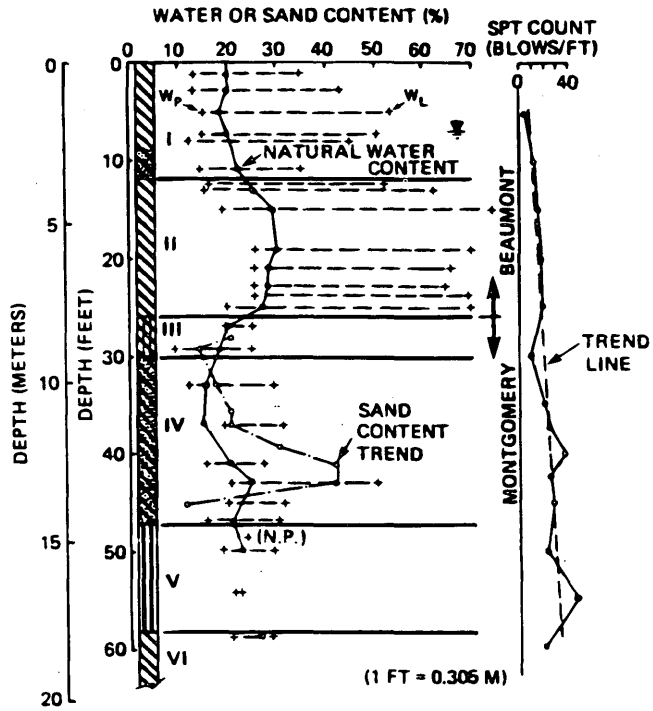

FIGURE 2 General profile of Beaumont-Montgomery sequence at Site A (*5*). Stratigraphy: I, very stiff gray and tan clay (CL-CH); II, stiff to very stiff red and light gray clay (CH); III, medium stiff light gray very silty clay (CL); IV, stiff to very stiff light gray and tan sandy clay with sand pockets (CL); V, dense red and light gray silt with clayey silt and sand layers (ML); VI, very stiff red and light gray clay (CL).

150 m, allowing relatively large and heavy structures to be constructed in the Houston area by taking advantage of the deep preconsolidation zone through the use of partially compensated rafts.

GENERAL ENGINEERING PROPERTIES

Two sites (Sites A and B, Figure 1) are examined that have been profiled geotechnically by various means, with emphasis on the National Geotechnical Experimentation Site (NGES) at the University of Houston, Site A. Site A is a microdelta depositional site within the Beaumont formation, whereas Site B is a backswamp site within the Beaumont formation near a natural levee. These sites represent the lower and upper limits, respectively, for theoretical preconsolidation in the region, and possibly in the Beaumont formation. A general profile for Site A is shown in Figure 2. The Beaumont-Montgomery contact is at a depth of about 8 m. At Site B, the contact appears to be at a depth of about 11 m. At both sites the piezometric surface is at a depth of about 2 m.

The mineralogy of the soils at the two sites is somewhat different, as characterized by the average index properties (I_p and w_L) in Table 1.

A profile of the OCR (OCR = maximum past vertical effective stress/present vertical effective stress) is presented in Figure 3 for both sites, as determined by relatively sparse data from Shelby tube samples using the indicated laboratory test methods. Individual values are shown only for Site A. The trend lines are strictly visual fits. More details on the interpretation of the laboratory test methods are presented by Mahar and O'Neill (*5*) and O'Neill et al. (*6*).

The resolution of test data is insufficient to delineate any difference in OCR at either site as one passes from the Beaumont into the Montgomery (Figure 3), despite the geological history and the differences in index properties.

UNDRAINED SHEAR STRENGTH

Typical stress difference/pore-water-pressure relations are shown in Figure 4 for anisotropically consolidated, saturated, undrained triaxial test specimens (CAU tests) from the Beaumont formation at Site A. Samples were trimmed horizontally and tested vertically in triaxial cells. σ_a represents axial stress (horizontal direction in ground) or stress in the direction of compressive loading. At the end of the consolidation stage, σ_a was equal to the estimated K_0, discussed later, times the present vertical effective stress, σ'_{vo}. σ_1 is lateral stress in the triaxial stress system, which was set equal to the average of σ'_2 and σ'_3 for the horizontal specimen, or $0.5(1 + K_0)$ σ'_{vo}. The test therefore models horizontal loading.

Stratum II soils (lower portion of the Beaumont, Figure 2) are more blocky than those in Stratum I (upper portion of the Beaumont) and so exhibit a more decided "knee" at lower axial strains (ϵ_a) than in Stratum I. Both soils are dilative beyond a major principal strain of about 1.5 percent.

TABLE 1 Index Properties at Sites A and B

	Beaumont			Montgomery		
		Avg Index Properties			Avg Index Properties	
Site	Depth Range (m)	I_p	w_L	Depth Range (m)	I_p	w_L
A	0–8	42	61	8–20	15	29
B	0–11	35	55	11–35	25	37

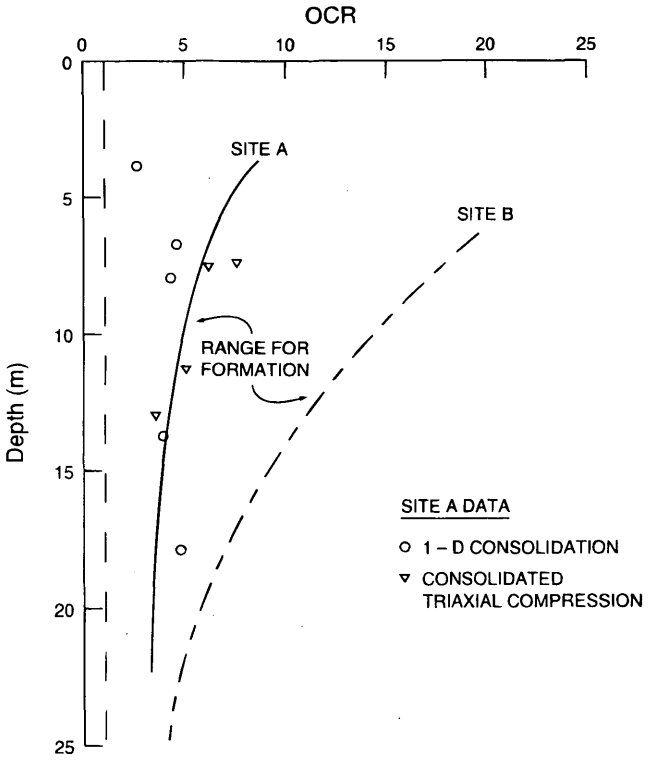

FIGURE 3 OCR-depth profiles at Sites A and B (*3,5*).

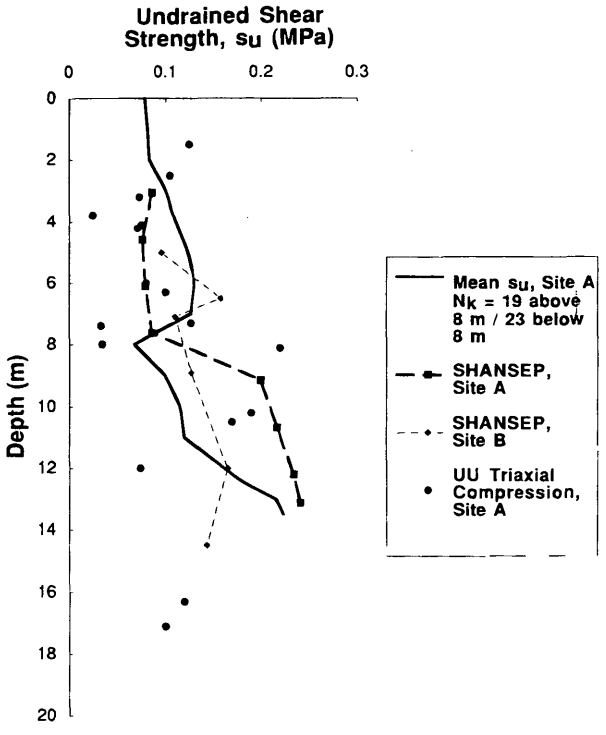

FIGURE 5 Relationship of undrained shear strength to depth at Sites A and B (*3,5*).

Undrained shear strength (s_u) is profiled by several methods at Site A in Figure 5. Also shown is a profile of s_u at Site B by the stress history and normalized soil engineering properties (SHANSEP) method (*3*). UU triaxial compression tests, in which the total, isotropic confining stress is equal to the total overburden stress, exhibit a wide variation in shear strength, reflecting the variable local joint structure and the presence of sand or silt seams. The SHANSEP method provides a marked improvement in consistency of s_u values at Site A, with the only major difference being that of the values below 8 m (within the Montgomery) from those above (within the Beaumont). At Site B, SHANSEP tests indicated higher s_us within the Beaumont than within the Beaumont at Site A, which is expected because of the differences in preconsolidation (capillary) pressures at the two sites, owing to their different microdepositional environments. In the upper Montgomery, the opposite effect is evident, possibly because the clay in the Montgomery has a higher I_p (is less weathered) at Site B.

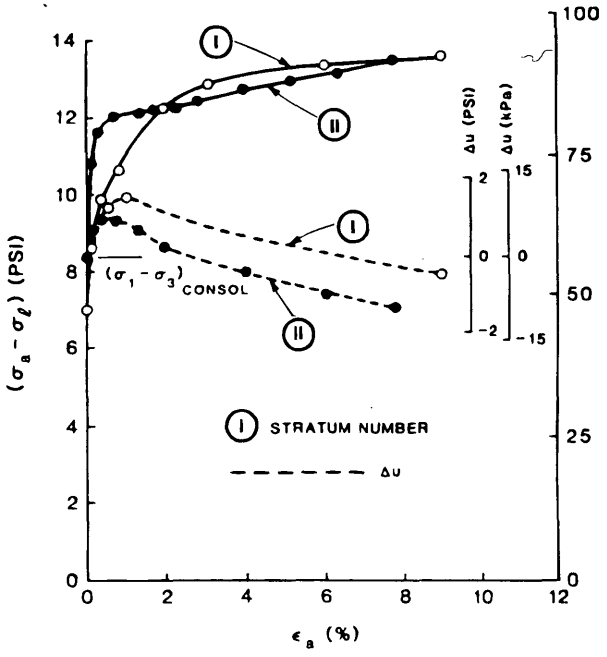

FIGURE 4 Typical stress-strain-pore-water pressure relations for Beaumont formation soils.

The most consistent routine procedure for profiling s_u at Site A appears to be the cone penetration test (CPT). The curve labeled "from mean q_c" shown in Figure 5 is an average s_u relation from 16 electronic CPT tests, all made within a zone 30 m square, using $s_u =$, where q_c is the cone tip resistance. Statistical properties of the variation among individual CPT soundings are discussed by O'Neill (*7*). A sense of that variability is shown later in this paper in the section on CPTU profiling. Note that the Beaumont-Montgomery contact is evident by a reduction in s_u at a depth of 8 m, where a thin zone of waterbearing silt exists atop the Montgomery.

A relationship between s_u and OCR at Site A for both the Beaumont and Montgomery formations is suggested in Figure 6, where w_L is liquid limit and σ'_{vo} is the present vertical effective stress, using total unit weights of 19.9 kN/m^3 in the Beaumont and 20.7 kN/m^3 in the Montgomery to compute σ'_{vo}. The data were developed from SHANSEP triaxial compression tests on K_0-consolidated, undrained (CU) vertically trimmed triaxial test specimens. w_L is used as a surrogate for ϕ', the effective angle of internal friction.

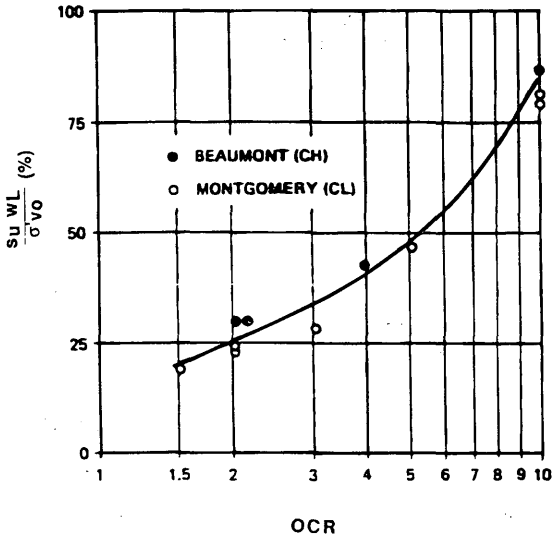

FIGURE 6 Nondimensional relationship between undrained shear strength and OCR for Beaumont and Montgomery formations (5).

Alternatively, Williams (*1*), using data from both Sites A and B, as well as from three other well-documented sites in the Houston area, determined a direct empirical relationship between s_u and OCR for the Beaumont formation:

$$s_u/\sigma'_{vo} = 0.24\text{OCR}^{0.6} \quad (1)$$

The range of validity of Equation 1 is $1 < \text{OCR} < 20$.

CPTU PROFILING

The CPTU test holds promise in profiling the Beaumont and Montgomery soils. Figure 7 shows a typical result for a CPTU test at Site A, in which pore-water pressures were measured on the sleeve just behind the cone tip on a 14-mm diameter, Fugro-type electronic cone. There is a clear change from positive to negative pore-water pressure (u) between Strata I (sandy, silty clay) and II (plastic clay), with relatively high values of $+u$ being observed in Stratum IA, which contained thin seams of waterbearing sand and silt. Again, the value of u changes from negative to positive when Stratum IV (very sandy clay) is reached, although the very top of the Montgomery (Stratum III) was not distinguished by a change of sign in u. Once interbedded silt layers were encountered below about 12 m, the sign of u became erratic.

Figure 8 shows results of a CPTU test made about 50 m from that shown in Figure 7 but in which the piezometric element was located on the cone tip. There are no negative pore-water pressures in this case, and it is difficult to distinguish strata, except that the Beaumont-Montgomery contact is clearly indicated by a sudden drop in u to near zero. The extreme variation in u may not reflect the variability of the soil but may instead be characteristic of continual plugging and unplugging of the piezo element by blocks of clay that attach and detach from the tip of the cone.

The cone with the piezo-sensing element on the tip appears to be the more appropriate for sensing pore-water pressures at Site A, as indicated by the results of dissipation tests shown in Figure 9. The sleeve element exhibits essentially instantaneous dissipation, possibly because of incomplete contact between the element and the stiff soil, whereas the tip element exhibits a dissipation pattern more representative of normal consolidation processes. If this hypothesis is correct, the magnitudes of the values of u presented in Figure 7 are probably incorrect, although the signs may be correct. Friction ratio (FR) values in Figures 7 and 8 are generally representative of

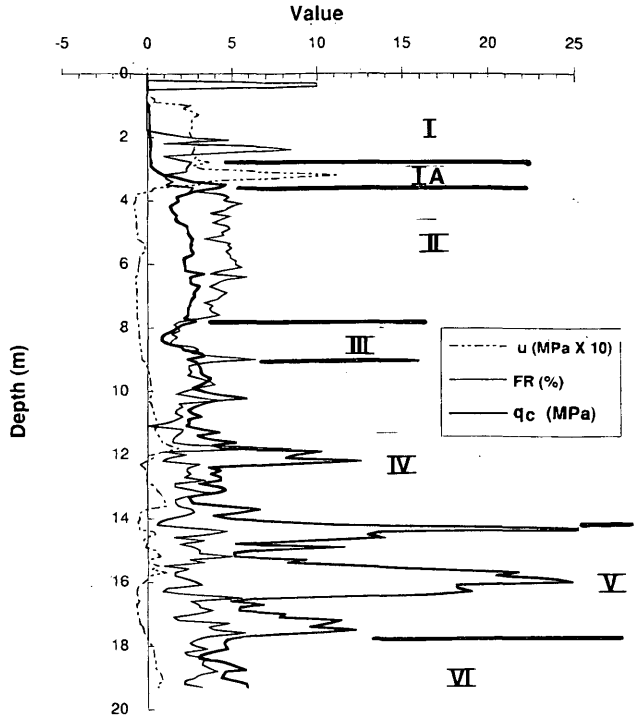

FIGURE 7 CPTU record No. 1 (Piezo element on sleeve), Site A.

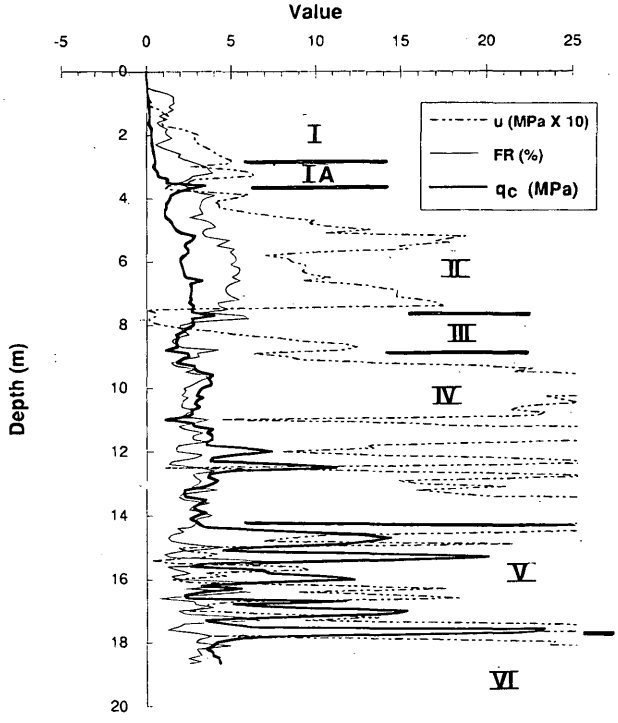

FIGURE 8 CPTU record No. 2 (Piezo element on tip), Site A.

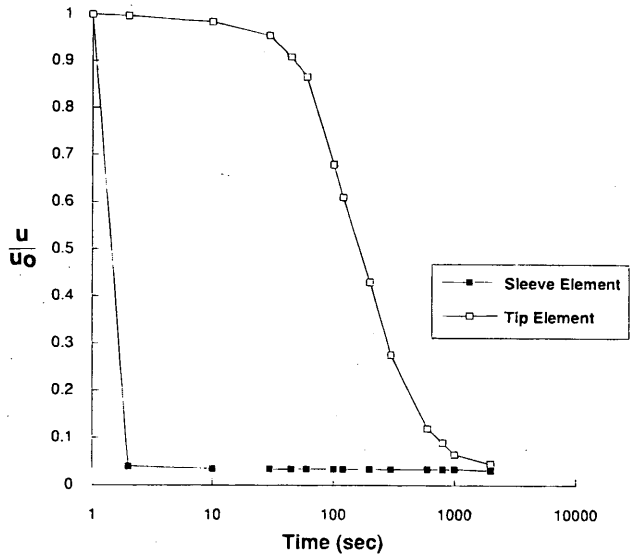

FIGURE 9 Pore-water pressure dissipation patterns: sleeve piezo element versus tip piezo element at depth of 8.6 m, Site A.

the soils described in Figure 2. q_c values at the two test locations shown in Figures 7 and 8 (50 m apart) are superimposed in Figure 10 to provide some indication of consistency. Coherence is high above a depth of about 12 m. The same general pattern can be observed below 12 m, but spike peaks vary slightly in elevation and more greatly in amplitude, indicating density variations in the silt and sand seams.

Mayne (*8*) proposed a practical method of determining a semicontinuous OCR profile from q_c readings, which has obvious potential advantages over profiling OCR using a few expensive laboratory tests, as follows:

$$\text{OCR} = [K\,(q_c - \gamma z)]/\sigma'_{vo} \tag{2}$$

where

K = site- or formation-specific constant of proportionality,

γz = total vertical stress at depth z, and

σ'_{vo} = present vertical effective stress in depth z.

In Figure 11 OCR was computed from Equation 2 at 0.1-m depth intervals from the data in Figure 8, using $K = 0.2$ (the optimum value for Site A) and then fitting the pointwise variable results with a second-order least squares regression line. All (four) computed OCR values above 20 were discarded.

Mayne and Bachus (*9*) have also suggested that OCR can be predicted from the CPTU u values. The u data from Figure 8 were plotted at 0.1-m depth intervals in Figure 12 and were then fit with a second-order least squares regression line. Mayne and Bachus, considering pore pressure generation from expanding cavity theory, propose that

$$\text{OCR} = a\,[(u/\sigma'_{vo}) - 1]^b \tag{3}$$

Factors a and b were shown to be 0.38 and 1.33 respectively from theory, and, using these values, Mayne and Bachus were able to profile OCR in the Yorktown formation in Virginia. At Site A the optimum values of a and b are 0.31 and 1.20, respectively, using the u values from the continuous, fitted relationship in Figure 12. Results of both the Mayne and Mayne-Bachus methods for Site A are shown in Figure 13. Both give generally similar results, and both

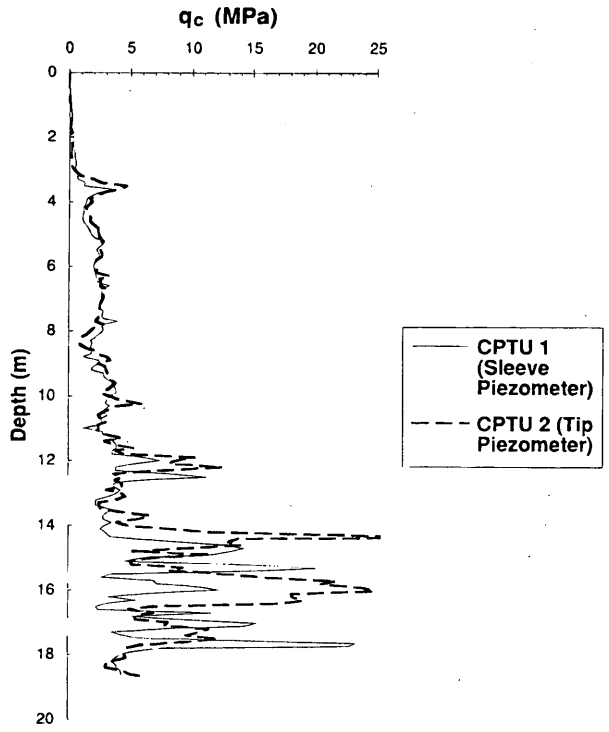

FIGURE 10 Comparison of q_c from CPTU records at Site A.

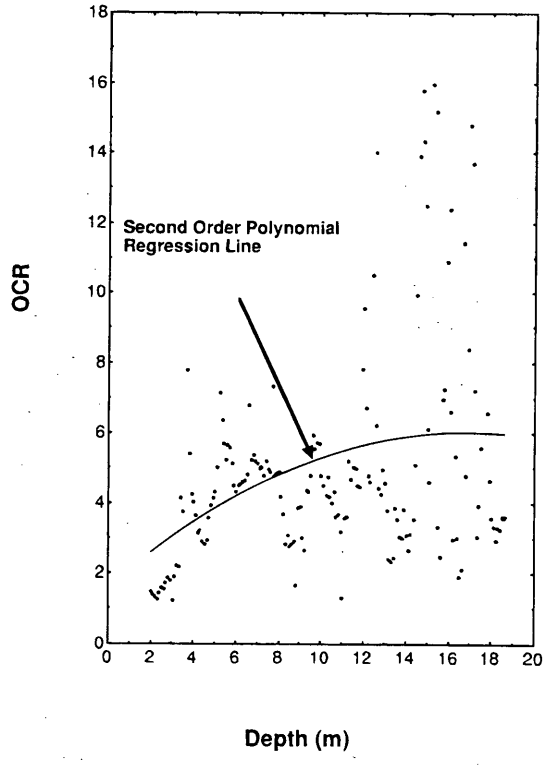

FIGURE 11 OCR versus depth from Mayne method using q_c from Figure 8.

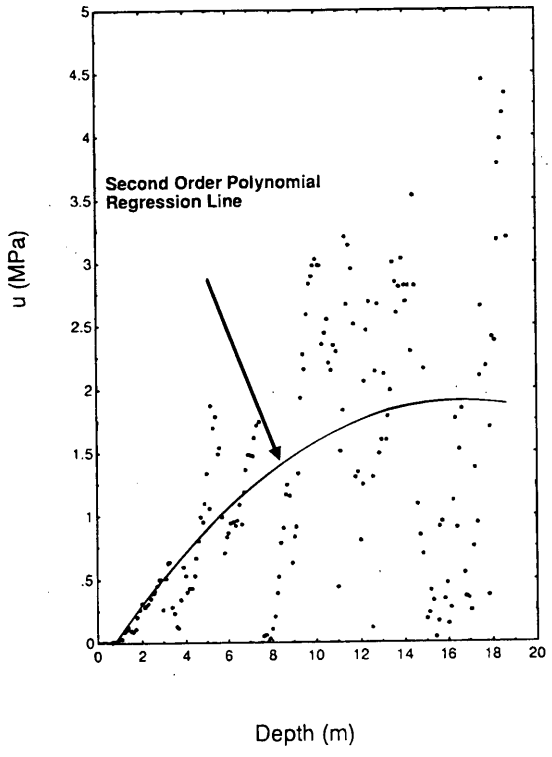

FIGURE 12 Fitted pore-water pressure for record in Figure 8.

provide a reasonable fit to the triaxial and one-dimensional consolidation test data, as fitted visually in Figure 3, but it is unclear at present which method is the more appropriate one.

COEFFICIENT OF EARTH PRESSURE AT REST (K_0)

K_0 has been estimated at Site A by numerous methods, as indicated in the legend to Figure 14. Results are from random positions around the site. The test locations for the two dilatometer soundings were at the extremities of the site, approximately 120 m apart, whereas most of the other tests were nearest DMT1. Interpretations of the dilatometer test (DMT) were in accordance with work by Marchetti (*10*). Good correspondence between DMT1 and DMT2 is observed except at the depth of 8 m, at the surface of the Montgomery formation, which indicates some degree of inconsistency at the unconformable contact. There is also general agreement in the patterns of K_0 between the DMT and the FHWA stepped blade (*11*), although the stepped blade is somewhat more variable. The self-boring pressuremeter test (SBPMT) (*6*) yielded two very high values (at 6 and 18 m), but otherwise was consistent with the other in situ tools.

The familiar correlation of Brooker and Ireland (*12*), based on OCR measured in the laboratory and or index properties, tends to provide a good fit of the directly measured values of K_0. The trend line for the computations of K_0 from the Brooker and Ireland method is shown in Figure 14.

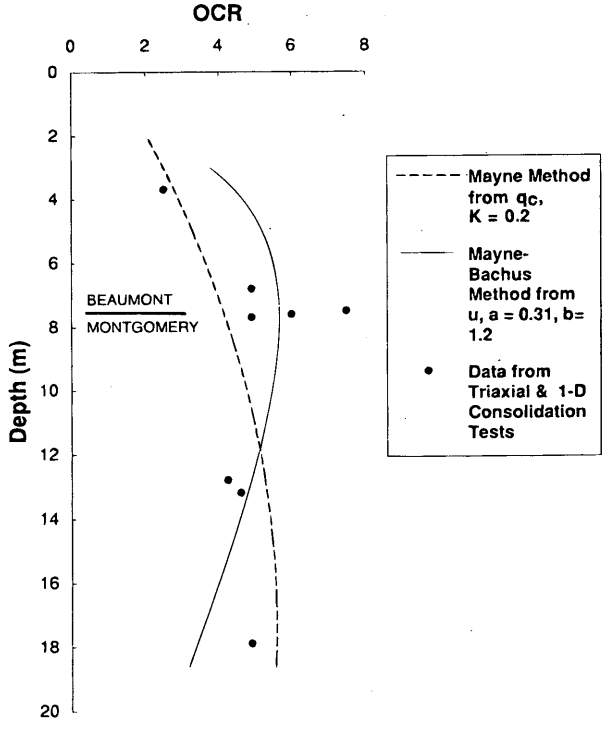

FIGURE 13 OCR versus depth at Site A: Mayne method, Mayne-Bachus method, and laboratory measurements.

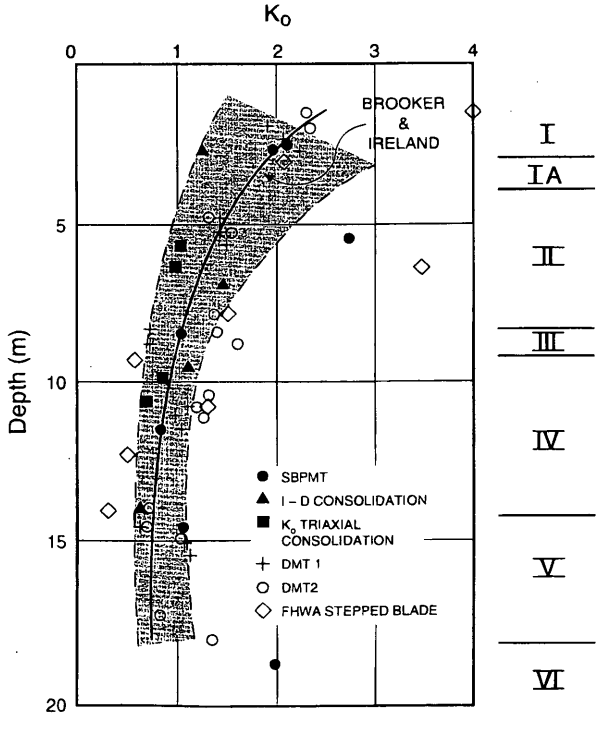

FIGURE 14 K_0 versus depth for Site A.

YOUNG'S MODULUS

Young's modulus (E) for undrained loading has been determined as a function of depth at Site A by several methods, as shown in Figure 15. For the DMT tests, E was taken to be equal to the dilatometer modulus E_d, assuming Poisson's ratio of the soil (ν) to be 0.33 (*10*). For the crosshole tests, the velocities of vertically polarized s-waves were measured to obtain shear modulus, which was converted to E by assuming ν to be 0.45. A similar value was used in converting pressuremeter modulus to E. In the triaxial tests, E was evaluated as the secant modulus at a principal stress difference equal to one-fifth of the peak principal stress difference. The various methods are generally consistent, except for the crosshole method, which gives values that are almost an order of magnitude higher than the other methods, as expected because of the small strains associated with crosshole testing.

E values determined from UU triaxial compression tests were highly erratic and are therefore not shown in Figure 15. By comparing a linear least squares fit of the values from Figure 15 (except crosshole) with the cone-generated s_u relation in Figure 5, one obtains

$$E/s_u = 206 + 1.4\,z\ (\text{m}) \qquad z < 20\ \text{m} \tag{4}$$

for Site A, where z is depth below the ground surface. Williams and Focht (*13*) have back-calculated from short-term settlement observations on 15 large raft-supported structures within the Houston area, in which the raft depth was at or below the Beaumont-Montgomery contact. Where the soil profile was predominantly clay, they found that

$$100 + 32\,z'\ (\text{m}) < E/s_u < 200 + 40\,z'\ (\text{m}) \tag{5}$$

where z' is depth below the raft (mean raft depth of about 10 m below the surface). The lower z-intercept values in Equation 5 may be due to effects of excavation, and the higher gradient with depth may be due to decreasing strain levels below the raft foundations, whereas in the in situ tests (Equation 4), relevant strain values remain approximately constant with depth.

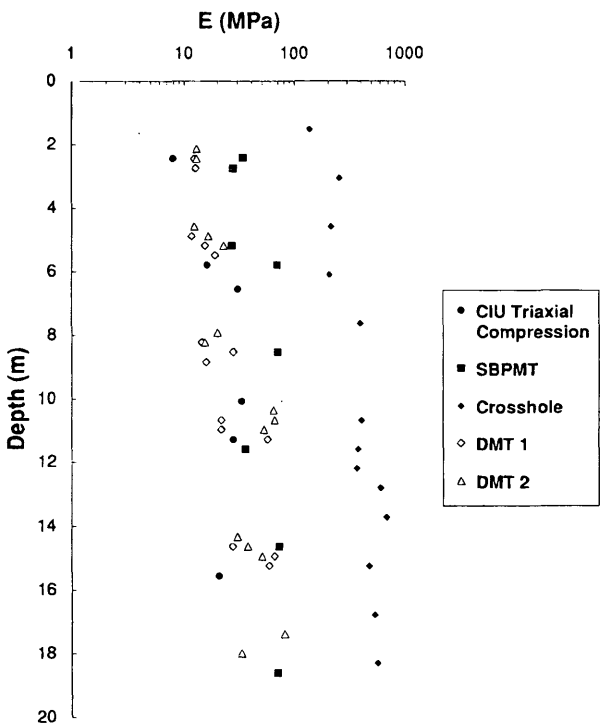

FIGURE 15 First-cycle Young's modulus versus depth, Site A.

CONCLUSIONS

The Beaumont-Montgomery sequence was deposited in a deltaic environment and was preconsolidated by desiccation. As such, the properties are complex and variable. Nonetheless, relatively clear estimations of mean s_u, OCR, K_0, and E are possible with sufficient investigation at a given site. However, mean properties change from site to site depending on the location of the site relative to ancient distributary channels. The most comprehensively studied property, OCR, is in the range of 3 to 7 below the piezometric surface at Site A, a pro-delta site within the upper (Beaumont) formation. Site B, a backswamp site in the upper formation several kilometers from Site A, indicated that values of OCR are two to three times as high. Corresponding average values of s_u from CPT records (Figure 5) are about 0.09 MPa in the upper formation at Site A and 0.11 MPa in the upper formation at Site B. Use of s_u to characterize shear strength in the lower (Montgomery) formation may not be entirely appropriate for most applications because of its sandy nature; however, s_u values from both q_c correlations and SHANSEP tests trend higher than those in the upper formation, approximately 0.1 to 0.2 MPa, although the OCR tends to be less in the lower formation.

Preliminary evidence indicates that CPTU profiling can be used to establish the OCR profile in the formations considered here, either with q_c readings or u readings for a cone with the piezo element on the tip. Piezocones can also possibly be used to identify stratum changes, but it is not clear whether the tip or sleeve piezo element is more appropriate for that task.

ACKNOWLEDGMENTS

Numerous agencies provided assistance to produce and provide the data reported here. They include Fugro Geosciences, Inc., McBride-Ratcliff and Associates, Southwestern Laboratories, Inc., University of Houston, University of Texas, Iowa State University, and Louisiana State University. Most of the data at the NGES (Site A) were acquired under several grants and contracts from the National Science Foundation and FHWA from 1979 to 1993.

REFERENCES

1. Rainwater, E. H., and R. P. Zingula, *Geology of the Gulf Coast and Central Texas*. Houston Geological Society, Houston, 1962.
2. Al-Layla, M. T. H. *Study of Certain Geotechnical Properties of Beaumont Clay*. Ph.D. thesis. Graduate College of Texas A and M University, Jan. 1970.
3. Williams, C. E. The Influence of Geology on the Behavior of Beaumont Formation Cohesive Soils. Presented at the Texas Section, ASCE, Meeting, San Antonio, Tex., 1987.

4. Georghiou, C., M. W. O'Neill, and O. I. Ghazzaly. Spatial Characterization of Expansive Clay. In *Transportation Research Record 1032*, TRB, National Research Council, Washington, D.C., 1986, pp. 8–15.
5. Mahar, L. J., and M. W. O'Neill. Geotechnical Characterization of Desiccated Clay. *Journal of Geotechnical Engineering*, ASCE, Vol. 109, No. 1, Jan. 1983, pp. 56–71.
6. O'Neill, M. W., R. A. Hawkins, and L. J. Mahar. Field Study of Pile Group Action, Final Report, Appendix C. *Report FHWA/RD-81/005*. FHWA, U.S. Department of Transportation, 1981.
7. O'Neill, M. W. Reliability of Pile Capacity Assessment by CPT in Overconsolidated Clay. In *Geotechnical Special Report 6: Use of In Situ Tests in Geotechnical Engineering*, ASCE S.P. Clemence, Ed., 1986, pp. 237–256.
8. Mayne, P. W. CPT Indexing of In Situ OCR in Clays. In *Geotechnical Special Report 6: Use of In Situ Tests in Geotechnical Engineering*. ASCE, S.P. Clemence, Ed., 1986, pp. 780–793.
9. Mayne, P. W., and R. C. Bachus. Profiling OCR in Clays by Piezocone Soundings. In *Penetration Testing*, (J. De Reuter, ed.) Balkema, Rotterdam, 1988, Vol. 2, pp. 857–864.
10. Marchetti, S. In Situ Tests by Flat Dilatometer. *Journal of the Geotechnical Engineering Division*, ASCE, Vol. 106, No. GT3, March, 1980, pp. 299–321.
11. Handy, R. L., B. Remmes, S. Moldt, A. J. Lutenegger, and G. Trott. In Situ Stress Determination by Iowa Stepped Blade. *Journal of the Geotechnical Engineering Division*, ASCE, Vol. 108, No. GT11, Nov. 1982, pp. 1405–1422.
12. Brooker, E. W., and H. O. Ireland. Earth Pressures at Rest Related to Stress History. *Canadian Geotechnical Journal*, Vol. II, No. 1, Feb. 1965, pp. 1–15.
13. Williams, C. E., and J. A. Focht III. Initial Response of Foundations on Stiff Clay. *Preprint 82-931*, ASCE Convention and Exhibit, New Orleans, Louisiana, October, 1982, 18 pp.